Conformational Analysis of Ferrocene-Containing Alcohols. A Density Functional Study of Weak OH···Fe Interactions

Valerije Vrček[†] and Michael Bühl*[,‡]

Faculty of Pharmacy and Biochemistry, University of Zagreb, HR-10000, Zagreb, Croatia, and Max-Planck-Institut für Kohlenforschung, Kaiser-Wilhelm-Platz 1, D-45470 Mülheim an der Ruhr, Germany

Received September 19, 2005

Optimized geometries and ν_{OH} stretching frequencies are reported for a set of monosubstituted ferrocenes, $Fe(C_5H_5)(C_5H_4R)$ [R = $(CH_2)_nOH$ (n = 1−4), CH(Me)OH, CH(*t*Bu)OH], at the BP86 level of density functional theory. In addition, NMR chemical shifts have been computed at the GIAO-B3LYP level. In all species studied, the most stable conformer is characterized by an OH···Fe moiety with Fe···H distances in the region between 2.61 and 2.95 Å, followed by conformers with OH···π interactions involving the C(ipso) atoms of the cyclopentadienyl ring. According to population and topological (Bader) analyses of the electron density, these conformers are stabilized by weak electrostatic interactions, rather than by true intramolecular hydrogen bonds. The ν_{OH} stretching frequencies are a very sensitive probe for the OH···Fe interaction, and the observed red-shift of this band relative to isomers with "free" OH bonds, which can exceed 100 cm^{-1}, is well reproduced computationally. When other H-bond acceptors are present, the intramolecular OH···Fe interaction cannot compete with intermolecular H-bond formation, as has been explicitly shown in a Car−Parrinello molecular dynamics (CPMD) simulation of $Fe(C_5H_5)(C_5H_4CH_2OH)$ in water. Compared to these unconstrained ferrocene-containing alcohols, somewhat stronger OH···Fe interactions can be present in *ansa* derivatives, e.g., in a [2]ferrocenophane derivative with a CH_2CH_2OH group, for which a bond path between Fe and the alcoholic H atom is found.

Introduction

Hydrogen bonds are remarkably variable in their strength. Interaction energies in Y−H···X systems can range from quite large values, with true multicenter bonding as one limit, down to very small numbers at the brink of perceptibility,[1] with zero as the obvious other limit. Metal centers in coordinatively saturated transition-metal complexes tend to be quite poor hydrogen-bond acceptors, even if they carry substantial electron density in occupied d-orbitals. The interaction between these metal centers with typical hydrogen-bond donors is usually weak, but can sometimes be observed[2] and has recently been counted among the "diverse world of unconventional hydrogen bonds".[2b] In ferrocene-containing alcohols, for instance, intramolecular OH···Fe interactions have been detected IR-spectroscopically.[3] Detailed knowledge of the nature and strength of these interactions is still rudimentary, despite a number of experimental and theoretical studies[4,5] directed toward that issue. Ferrocene is basic enough to be protonated by strong acids, and evidence is accumulating that the iron atom is one plausible site of protonation.[6] Thus, it is reasonable to assume that the metal could indeed act as a potential hydrogen-bond acceptor toward protic substrates, possibly competing for H-bonding with other electron-rich sites, such as the π-systems of the aromatic ligands. Indeed, a mixture of species with "free" OH groups and with intramolecular OH···Cp or OH···Fe interactions has been invoked to interpret IR spectra of ferrocene-containing alcohols.[3] These species are thus ideally suited to study this type of interaction.

Among the plethora of monosubstituted metallocenes, ferrocene-containing alcohols are of considerable interest in their own right, as they are precursors to ferrocene-stabilized carbocations,[7] intermediates in the synthesis of chiral ligands for asymmetric catalysis,[8] or redox-active probes of micelles,[9] to name but a few applications. These species show a variety of intramolecular interactions and hydrogen-bonding motifs, and their conformational flexibility allows for competition between intra- and intermolecular effects. We now present a systematic study of such effects in suitable ferrocene-containing alcohols, using the modern tools of density functional theory (DFT). Special attention is called to conformational analysis, to the assessment of intramolecular OH···Fe interactions, and to the requirements for their occurrence.

The target molecules in this study, sketched in Chart 1, range from the simple ferrocenylmethanol (**1**) to α-ferrocenylcarbinols with bulkier side chains (**2**, **3**), and to ω-derivatives with linear

* To whom correspondence should be addressed. Fax: 49 + 208-306-2996. E-mail: buehl@mpi-muelheim.mpg.de.

† University of Zagreb.

‡ Max-Planck-Institut für Kohlenforschung.

(1) Desiraju, G.; Steiner, T. In *The Weak Hydrogen Bond In Structural Chemistry and Biology*; Oxford University Press, 2001.

(2) (a) Shubina, E. S.; Belkova, N. V.; Epstein, L. M. *J. Organomet. Chem.* **1997**, *537*, 17−29. (b) Belkova, N. V.; Shubina, E. S.; Epstein, L. M. *Acc. Chem. Res.* **2005**, *38*, 624−631.

(3) (a) Baker, A. W.; Bublitz, D. E. *Spectrochim. Acta* **1966**, *22*, 1787−1799. (b) Trifan, D. S.; Bacskai, R. *J. Am. Chem. Soc.* **1960**, *82*, 5010−5011.

(4) (a) Shubina E. S.; Epstein L. M.; Timofeeva, T. V.; Struchkov, Yu. T.; Kreindlin, A. Z. Fadeeva, S. S.; Rybinskaya, M. I. *J. Organomet. Chem.* **1988**, *346*, 59−66. (b) Shubina Y. S.; Epstein L. M. *J. Mol. Struct.* **1992**, *265*, 367−384.

(5) Orlova, G.; Scheiner, S. *Organometallics* **1998**, *17*, 4362−4367.

(6) See e.g.: (a) McKee, M. L. *J. Am. Chem. Soc.* **1993**, *115*, 2818−2824. (b) Karlsson, A.; Broo, A.; Ahlberg, P. *Can. J. Chem.* **1999**, *77*, 628−633. (c) Bühl, M.; Grigoleit, S. *Organometallics* **2005**, *24*, 1516−1527, and references therein.

(7) (a) Olah, G. A.; Liang, G. *J. Org. Chem.* **1975**, *40*, 1849−1850. (b) Müller, T. J. J. *Eur. J. Org. Chem.* **2001**, *11*, 2021−2033.

(8) (a) Togni, A. In *Metallocenes: Synthesis and Reactivity*, Togni, A., Halterman, R. L., Eds.; Wiley-VCH: Weinheim, 1998; Vol. 2, p 685. (b) Schwink, L.; Knochel, P. *Chem. Eur. J.* **1998**, *4*, 950−968.

(9) Zu, X.; Rusling, J. F. *Langmuir* **1997**, *13*, 3693−3699.

10.1021/om050810p CCC: $33.50 © 2006 American Chemical Society
Publication on Web 12/06/2005

Chart 1

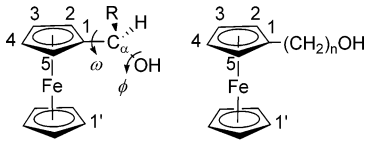

1 R = H
2 R = Me
3 R = *t*-Bu

1 n = 1
4 n = 2
5 n = 3
6 n = 4

aliphatic chains as variable spacer between metal and OH group (**4**−**6**).

The latter are of interest because elongation of this side chain influences not only chemical[3,10] but also biological properties of ferrocene-containing alcohols. It has been demonstrated that antineoplastic and cytostatic properties for potential cancer treatment change with increasing side chain length in monosubstituted ferrocenyl alcohols.[11] In addition, the methylene group linker was used for covalent attachment of ferrocene and different carbohydrates, thus enabling a comparative study of these bioconjugates.[12]

Computational Details

Geometries were fully optimized (without symmetry, unless otherwise noted) at the RI-BP86 level as implemented in the G03 program,[13] employing the exchange and correlation functionals of Becke[14] and Perdew,[15] respectively, together with a fine integration grid (75 radial shells with 302 angular points per shell), the augmented Wachters' basis[16] on Fe (8s7p4d), 6-31G(d) basis[17] on all other elements (denoted AE1 in previous work), and suitable auxiliary basis sets for the fitting of the Coulomb potential.[18] This and comparable DFT levels have proven quite successful for transition-metal compounds and are well suited for the description of structures, energies, vibrational frequencies, and other properties of organometallics in general, and metallocene compounds in particular.[19,20] Harmonic frequencies were computed from analytical second derivatives. Test calculations for selected substrates at the RI-BP86 and at the BP86 level (i.e., without density fitting) confirmed that geometrical parameters and harmonic vibrations were essentially identical with both approaches. In all calculations the ferrocene moiety maintained its eclipsed conformation.

Natural population analyses and topological (Bader) analyses[21] of the RI-BP86/AE1 total electron densities have been performed using the NBO[22] routines in Gaussian 03 and the Morphy program,[23] respectively.

Test calculations for the ferrocene−water complex indicated that interaction energies suffer from substantial basis-set superposition error (BSSE) at that level. This error is significantly reduced when the 6-31+G(d,p) basis, denoted AE1(+), is employed on the OH group (e.g., for ferrocene + water the raw interaction energy with this augmented basis is −1.9 kcal/mol, which is reduced to −1.2 kcal/mol after correction for BSSE with the Counterpoise method[24]). These interaction energies, as well as the relative energies of all conformers of complex **1**, are virtually identical when the molecules are fully optimized with this augmented AE1(+) basis, or when just single-point energies are calculated for the BP86/AE1 geometries. We thus adopted the latter protocol and report AE1(+) single-point energies throughout (i.e., at the BP86/AE1(+)//BP86/AE1 level).

For the rotamers of **1**, additional optimizations were performed at the B3LYP/AE1 level[25] for the gas phase and at the BP86/AE1 level employing the polarizable continuum model (PCM) of Tomasi and co-workers[26] (using the parameters of water), followed by AE1(+) single-point calculations at the same respective level.

Molecular dynamics (MD) simulations were performed using the Car−Parrinello scheme[27] as implemented in the CPMD program.[28] The BP86 functional was used, together with norm-conserving Troullier−Martins pseudopotentials in the Kleinman−Bylander form.[29] Periodic boundary conditions were imposed using cubic supercells with box sizes of 13.0 Å. Kohn−Sham orbitals were expanded in plane waves up to a kinetic energy cutoff of 80 Ry. In the MD simulations a fictitious electronic mass of 600 au and a time step of 0.121 fs were used. To increase the simulation time step, hydrogen was substituted with deuterium. Microcanonical simulations were performed for a total of 2 ps at ca. 300 K in the gas phase, after instantaneous heat-up starting from the equilibrium structures, which were fully optimized using the same methodology (denoted CP-opt). For the simulation of **1a** in water, the box was filled with 61 water molecules, rendering a density of 1.0. The

(10) Enantioselective acetylation of ferrocene-containing alcohols: Dakovic, S.; Lapic, J.; Rapic, V. *Biocatal. Biotransform.* **2003**, *21*, 291−295. Preparation of ferrocenyl diols: Jary, W. G.; Baumgartner, J. *Tetrahedron: Asymm.* **1998**, *9*, 2081−2085. Electrochemical properties: Davis, W. L.; Shago, R. F.; Langner, E. H. G.; Swarts, J. C. *Polyhedron* **2005**, *24*, 1611−1616.

(11) Swarts, J. C.; Swarts, D. M.; Maree, D. M.; Neuse, E. W.; La Madeleine, C.; van Lier, J. E. *Anticancer Res.* **2001**, *21*, 2033−2037.

(12) van Staveren, D. R.; Metzler-Nolte, N. *Chem. Rev.* **2004**, 104, 5931−5985.

(13) Frisch, M. J.; Trucks, G. W.; Schlegel, H. B.; Scuseria, G. E.; Robb, M. A.; Cheeseman, J. R.; Montgomery, J. A., Jr.; Vreven, T.; Kudin, K. N.; Burant, J. C.; Millam, J. M.; Iyengar, S. S.; Tomasi, J.; Barone, V.; Mennucci, B.; Cossi, M.; Scalmani, G.; Rega, N.; Petersson, G. A.; Nakatsuji, H.; Hada, M.; Ehara, M.; Toyota, K.; Fukuda, R.; Hasegawa, J.; Ishida, M.; Nakajima, T.; Honda, Y.; Kitao, O.; Nakai, H.; Klene, M.; Li, X.; Knox, J. E.; Hratchian, H. P.; Cross, J. B.; Bakken, V.; Adamo, C.; Jaramillo, J.; Gomperts, R.; Stratmann, R. E.; Yazyev, O.; Austin, A. J.; Cammi, R.; Pomelli, C.; Ochterski, J. W.; Ayala, P. Y.; Morokuma, K.; Voth, G. A.; Salvador, P.; Dannenberg, J. J.; Zakrzewski, V. G.; Dapprich, S.; Daniels, A. D.; Strain, M. C.; Farkas, O.; Malick, D. K.; Rabuck, A. D.; Raghavachari, K.; Foresman, J. B.; Ortiz, J. V.; Cui, Q.; Baboul, A. G.; Clifford, S.; Cioslowski, J.; Stefanov, B. B.; Liu, G.; Liashenko, A.; Piskorz, P.; Komaromi, I.; Martin, R. L.; Fox, D. J.; Keith, T.; Al-Laham, M. A.; Peng, C. Y.; Nanayakkara, A.; Challacombe, M.; Gill, P. M. W.; Johnson, B.; Chen, W.; Wong, M. W.; Gonzalez, C.; Pople, J. A. *Gaussian 03*, revision C.02; Gaussian, Inc.: Wallingford, CT, 2004.

(14) Becke, A. D. *Phys. Rev. A* **1988**, *38*, 3098−3100.

(15) (a) Perdew, J. P. *Phys. Rev. B* **1986**, *33*, 8822−8824. (b) Perdew, J. P. *Phys. Rev. B* **1986**, *34*, 7406.

(16) (a) Wachters, A. J. H. *J. Chem. Phys.* **1970**, *52*, 1033−1036. (b) Hay, P. J. *J. Chem. Phys.* **1977**, *66*, 4377−4384.

(17) (a) Hehre, W. J.; Ditchfield, R.; Pople, J. A. *J. Chem. Phys.* **1972**, *56*, 2257−2261. (b) Hariharan, P. C.; Pople, J. A. *Theor. Chim. Acta* **1973**, *28*, 213−222.

(18) Generated automatically according to the procedure implemented in Gaussian 03.

(19) See for instance: Koch, W.; Holthausen, M. C. *A Chemist's Guide to Density Functional Theory*; Wiley-VCH: Weinheim, 2000, and the extensive bibliography therein.

(20) (a) Ziegler, T. *Can. J. Chem.* **1995**, *73*, 743−761. (b) Mayor-Lopez, M. J.; Weber, J.; Mannfours, B.; Cunningham, A. F., Jr. *Organometallics* **1998**, *17*, 4983−4991. (c) Berces, A.; Ziegler, T. *Top. Curr. Chem.* **1996**, *182*, 41−85.

(21) Bader, R. F. W. *Atoms in Molecules*; Oxford Press: New York, 1990.

(22) Reed, A. E.; Curtiss, L. A.; Weinhold, F. *Chem. Rev.* **1988**, *88*, 899−926.

(23) Popelier, P. L. A. *Comput. Phys. Commun.* **1996**, *93*, 212−240.

(24) Boys, S. F.; Bernardi, F. *Mol. Phys.* **1970**, *19*, 553−566.

(25) (a) Becke, A. D. *J. Chem. Phys.* **1993**, *98*, 5648−5642. (b) Lee, C.; Yang, W.; Parr, R. G. *Phys. Rev. B* **1988**, *37*, 785−789.

(26) As implemented in G 03: (a) Barone, V.; Cossi, M.; Tomasi, J. *J. Comput. Chem.* **1998**, *19*, 404−417. (b) Cossi, M.; Scalmani, G.; Rega, N.; Barone, V. *J. Chem. Phys.* **2002**, *117*, 43−54. (c) Cossi, M.; Crescenzi, O. *J. Chem. Phys.* **2003**, *19*, 8863−8872.

(27) Car, R.; Parrinello, M. *Phys. Rev. Lett.* **1985**, *55*, 2471−2474.

(28) Hutter, J.; Alavi, A.; Deutsch, T.; Bernasconi, M.; Goedecker, S.; Marx, D.; Tuckerman, M.; Parrinello, M. *CPMD* Version 3.3a; Max-Planck-Institut für Festkörperforschung and IBM Research Laboratory (1995−1999).

(29) (a) Troullier, N.; Martins, J. L. *Phys. Rev. B* **1991**, *43*, 1993−2006. (b) Kleinman, L.; Bylander, D. M. *Phys. Rev. Lett.* **1982**, *48*, 1425−1428.

Chart 2

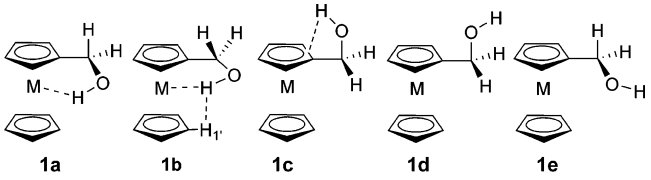

system was equilibrated for 0.5 ps maintaining a temperature of 300 (±50) K via velocity rescaling and was then propagated without constraints (NVT ensemble) for 2.5 ps.

Magnetic shieldings σ were computed at the B3LYP[25] level for the RI-BP86 equilibrium geometries, employing GIAOs (gauge-including atomic orbitals)[30] and basis II′, i.e., the augmented Wachters basis[19] on Fe, IGLO-basis II,[31] which is essentially of polarized triple-ζ quality, on C and O, and IGLO-DZ basis[31] on hydrogen. Chemical shifts were calculated relative to ferrocene (^{57}Fe, ^{13}C, and ^{1}H magnetic shieldings −4372.8, 106.2, and 28.1 ppm at the same level), and the ^{13}C and ^{1}H chemical shifts were converted to the usual standard, TMS, using the experimental $\delta(^{13}C)$ and $\delta(^{1}H)$ values of ferrocene, 67.8 and 4.2 ppm, respectively.[32] This level has been shown to perform very well for transition-metal chemical shifts, including ^{57}Fe, where further enlargement of the basis set in the NMR part has afforded only minor changes in the computed values.[33]

For comparison, computations for selected Ru analogues were performed using the methods and basis sets described in ref 34 involving BP86 optimizations with the Stuttgart−Dresden relativistic core potential on Ru[35] and 6-31G(d) on the ligands, single-point energy calculations employing 6-31+G(d,p) on the OH group, and NMR computations at the B3LYP/II′ level using a contracted, all-electron well-tempered Huzinaga basis on Ru.[36]

Ferrocenylmethanol

At the BP86 level of theory three different rotational isomers can be located for ferrocenylmethanol, namely, **1a**, **1c**, and **1d** (Chart 2). Additionally, the carbinol group is free to rotate about the central C_1-C_α bond to give the fourth rotational isomer, **1e**.[37] To our knowledge, the ferrocenylmethanol conformers **1a**, **1c**, and **1e** were not described previously.[38] We have also located a C_s-symmetrical structure, **1b**, which is characterized by one imaginary frequency (166.6i cm^{-1}). This transition structure is associated with the simultaneous rotation of the carbinol moiety and the OH group about the C−C and C−O bonds, respectively, converting **1a** into its enantiomer, and is calculated 2.1 kcal/mol above **1a**. Key geometrical parameters and relative energies of all species **1a**−**1e** are collected in Table 1. The relative stabilities are further assessed by means of full optimizations using a different density functional and a surrounding polarizable continuum mimicking a polar solvent (see below). In all cases, similar relative energies and the same sequence are obtained for the minima, except for the PCM data, where **1c** and **1d** switch their relative order.

Table 1. Torsional Angles (deg), OH-Stretching Frequencies (cm^{-1}), and Relative Energies (kcal/mol) for Ferrocenylmethanol Rotational Isomers Calculated at the BP86 Level

rotamer	ω^a	ϕ	$\nu_{OH}{}^b$	ΔE (BP86)	ΔE (B3LYP)^c	ΔE (PCM)^d
1a	−142.5	46.4	3579	0	0	0
			3579^e			
1b	−90.9	0.0	3538	2.1	2.4	1.4
1c	94.6	−53.9	3615	0.4	0.4	0.6
			3620^e			
1d	88.3	−179.9	3630	1.9	0.8	0.2
			3635^e			
1e	−146.9	−168.9	3615	2.3	1.1	2.2

^{a} Angles defined for the torsion about $C_2-C_1-C_\alpha-O$ (ω) and $C_1-C_\alpha-O-H$ (ϕ) (numbering defined in Chart 1). ^{b} Experimental numbers in italics. ^{c} Optimized at the B3LYP level (using the same basis sets as in the BP86 optimizations and single-point energies). ^{d} BP86 level; $\epsilon = 78.39$ ^{e} Dilute CH_2Cl_2 solution, from ref 3a.

The particular conformations of **1a** and **1c** are well suited for a possible stabilization by OH···Fe and OH···π intramolecular interactions, which are absent in the rotational isomers **1d** and **1e**. The optimized salient distances in the former, d(OH···Fe) = 2.949 Å in **1a** and d(OH···C$_1$) = 2.554 Å in **1c**,[39] already betray weak, if any, direct intramolecular H-bonding in these molecules (see below for more detailed analysis). The symmetrical transition structure **1b**, characterized by a short OH···H^1 distance of 1.933 Å, could be consistent with intramolecular dihydrogen bonding (see, however, below), an interaction not frequently observed in ferrocene chemistry.

In a conformational analysis based on molecular mechanics and a classical force field it was suggested that the OH···Fe interaction in ferrocenylmethanol could not be formed because the conformation with the OH group rotated toward the Fe atom did not correspond to a minimum on the potential energy surface.[4] On the contrary, we find that the structure in which the hydroxyl group is rotated toward the Fe atom (**1a**) is the most stable conformer (Table 1), both in the gas phase (BP86 and B3LYP levels) and in the solvent model (PCM-BP86; ϵ = 78.39; see below, however, for discussion of specific solute−solvent interactions). This discrepancy between MM and DFT results may be due to the inappropriate use of the MM method for conformational analysis of ferrocenyl carbinols.

Whereas in protic solvents and in the solid state[40] the intermolecular interactions of the OH group of the ferrocenylmethanol with other H-bond acceptors are energetically more favorable, in nonpolar solvents (CCl_4, cyclohexane) under high-dilution conditions, which exclude self-association, as well as in the gas phase, the OH···Fe and OH···π intramolecular interactions become operative. These two types of intramolecular

(30) (a) Ditchfield, R. *Mol. Phys.* **1974**, *27*, 789−807. (b) Wolinski, K.; Hinton, J. F.; Pulay, P. *J. Am. Chem. Soc.* **1990**, *112*, 8251−8260. GIAO-DFT implementation: (c) Cheeseman, J. R.; Trucks, G. W.; Keith, T. A.; Frisch, M. J. *J. Chem. Phys.* **1996**, *104*, 5497−5509.

(31) Kutzelnigg, W.; Fleischer, U.; Schindler, M. In *NMR Basic Principles and Progress Vol. 23*; Springer-Verlag: Berlin, 1990; pp 165−262.

(32) For experimental ^{57}Fe NMR data: Haslinger, E.; Robin, W.; Schloegel, K.; Weissensteiner W. *J. Organomet. Chem.* **1981**, *218*, C11. For experimental ^{13}C and ^{1}H NMR data: Spectral Database for Organic Compounds SDBS, accessed at http://www.aist.go.jp.

(33) Bühl, M. *Chem. Phys. Lett.* **1997**, *267*, 251−257.

(34) Bühl, M.; Gaemers, S.; Elsevier, C. J. *Chem. Eur. J.* **2000**, *6*, 3272−3280.

(35) Andrae, D.; Häussermann, U.; Dolg, M.; Stoll, H.; Preuss, H. *Theor. Chim. Acta* **1990**, *77*, 123−141.

(36) Huzinaga, S.; Klobukowski, M. *J. Mol. Struct.* **1988**, *167*, 1−210.

(37) The OH group in **1a** may rotate about the C−O bond to give one more rotamer, but during the geometry optimization this rotamer converged back to **1a**.

(38) It was reported that there was no minimum found that corresponds to structure **1a** (M = Fe). See ref 5.

(39) These distances are somewhat sensitive to the basis set employed in the optimization; e.g., when optimized at BP86/AE1(+), d(Fe···HO) = 2.978 Å is obtained for **1a**. The nonaugmented AE1 basis, which we used for the subsequent optimizations, is thus likely to underestimate the OH···Fe distance somewhat in absolute terms; our conclusions are based on relative trends, however, which should be much less affected by this issue.

(40) Shubina, E. S.; Epstein, L. M.; Yanovsky, A. I.; Timofeeva, T. V.; Struchkov, Yu. T.; Kreindlin, A. Z. Fadeeva, S. S.; Rybinskaya, M. I. *J. Organomet. Chem.* **1988**, *345*, 313−320.

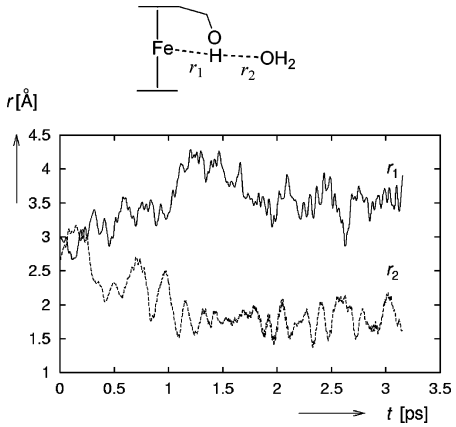

Figure 1. Evolution of OH···Fe (r1) and OH···OH_2 (r2) distances in a CPMD simulation starting from **1a** immersed in aqueous solution.

interactions are in competition with each other, stabilizing either structure **1a** or **1c**, respectively.

A few structures of monosubstituted ferrocenylcarbinols have been determined by X-ray crystallography;[41] in none of these is there evidence for intramolecular bonding of the OH group to the metal atom or a cyclopentadienyl ring in the solid. There is a competition between *intra*molecular OH···M interactions with stronger *inter*molecular hydrogen bonds, which depends on the proton-accepting abilities of the metal and other potential acceptors, in particular the O atom of the alcohol moiety in neighboring carbinol molecules.[42] In the case of ferrocenes, there is a clear preference for such intermolecular hydrogen bonds, but for more basic metal atoms, such as ruthenium or osmium analogues, the intramolecular OH···M interactions can successfully compete with intermolecular hydrogen bonds, even in the solid state.[2a]

To probe the stability of the intramolecular OH···Fe interaction in the presence of other strong hydrogen-bond acceptors, we have performed CPMD simulations of **1a** immersed in a box of liquid water. As expected, the alcoholic proton is rapidly drawn away from the metal toward the O atom of a water molecule from the bulk. This process is monitored in Figure 1, a plot of the salient distances involving this proton. Within ca. 1 ps (i.e., in a period arguably still counting as equilibration), one water molecule approaches within H-bonding distance (dashed line in Figure 1), while the distance to the metal (solid line) is significantly elongated.

This elongation is mainly a consequence of a rotation of the OH bond in **1a** around the $C_\alpha-O$ axis toward the incoming water molecule, resulting in a dihedral ϕ oscillating around ca. $-60°$ in solution. Interestingly, in the gas phase such a conformation appears to be unstable, as an attempted optimization collapsed to **1a**.

In a CPMD simulation in the gas phase, in contrast, **1a** remained stable for at least 2 ps, without showing any conformational changes. Likewise, no spontaneous rotations around C_1-C_α or $C_\alpha-O$ bonds were observed in a 4 ps CPMD simulation of gaseous **1c**, indicating that interconversion of the rotamers is an activated process happening on a longer time scale.

Chart 3

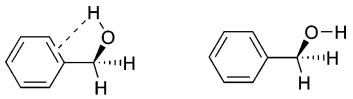

7a **7b**

IR and NMR Properties

The apparent stabilization of isomers **1a** and **1c** with putative OH···Fe and OH···π interactions is weak, as judged from the relative energies of rotamers **1e** and **1d** with "free" OH (i.e., **1e** is ca. 2 kcal/mol higher than **1a**, and **1d** is ca. 1 kcal/mol above **1c**, cf. Table 1). Nevertheless, there is IR and NMR spectroscopical evidence for the presence of such intramolecular interactions, apparent from measurable changes in spectral properties of ferrocenylmethanol and related compounds.

It has been shown that three distinct ν_{OH} bands can be observed in IR spectra of several ferrocenyl primary alcohols in concentrations sufficiently dilute to preclude intermolecular associations (<0.005 M).[3] In the case of ferrocenylmethanol the O−H stretching vibrations at 3635, 3620, and 3579 cm^{-1} have been assigned to the "free" OH group (structures **1d** and **1e**), the OH group interacting with the ferrocenyl π-electrons (**1c**), and the OH group interacting with the metal (**1a**), respectively. This red-shift of up to 56 cm^{-1} in IR spectrum of ferrocenylmethanol is well reproduced computationally at the BP86 level. The corresponding computed (unscaled) vibrational frequencies in the ν_{OH} region are 3630, 3615, and 3579 cm^{-1} for **1d**, **1c**, and **1a**, respectively, which is in excellent agreement with the experimental results (Table 1). The red-shift in the OH-stretching frequencies, on passing through the series of rotamers **1d**, **1c**, and **1a**, is also accompanied by a decrease in the corresponding computed force constants. In the rotamer **1d** the calculated force constant is 827 N/m,[43] whereas in rotamers **1a** and **1c** the OH bonds are weakened, as judged by a reduction in the corresponding force constants (803 and 820 N/m, respectively), through OH···Fe and OH···π interactions, respectively. These data suggest that these intramolecular interactions are weak, but relative differences in strength are still measurable.

From the calculated enthalpies for the interaction of the hydroxyl group with the ferrocenyl π-electrons and the d-orbitals of iron it was deduced that the iron-bonded form is 0.6 kcal/mol more stable than the π-bonded form.[3] At the BP86 and B3LYP levels **1a** is calculated to be 0.4 kcal/mol more stable than **1c** (Table 1), again in a very good agreement with experimental findings.

The assignment of the IR bands of ferrocenylmethanol to the corresponding isomer is straightforward, particularly when compared with benzyl alcohol (**7**).[44] The orientation of the OH group with respect to the aromatic ring in benzyl alcohol is interesting in view of an intramolecular OH···π interaction (Chart 3). The same mode of interaction also stabilizes isomer **1c** of ferrocenylmethanol (Chart 2). It has been shown that benzyl alcohol exhibits two stable conformations, the "gauche" form **7a** with the OH group oriented toward the phenyl plane,

(41) (a) Nataro, C.; Cleaver, W. M.; Landry, C. C.; Allen, C. W. *Polyhedron* **1999**, *18*, 1471−1473. (b) Glidewell, C.; Klar, R. B.; Lightfoot, P.; Zakaria, C. M.; Ferguson, G. *Acta Crystallogr., Sect. B: Struct. Sci.* **1996**, *52*, 110−121. (c) Yiwei L.; Ferguson, G.; Glidewell, C.; Zakaria, C. M. *Acta Crystallogr., Sect. C: Cryst. Struct. Commun.* **1994**, *50*, 857−861.

(42) The most common type of hydrogen bonds in the solid state is intermolecular hydrogen bonding of the OH···O type. See: Braga, D.; Grepioni, F.; Sabatino, P.; Desiraju, G. R. *Organometallics* **1994**, *13*, 3532−3543.

(43) 1 mDyne/Å = 100 N/m.

(44) The electronic similarity of phenyl and ferrocenyl rings is stressed by the ν_{OH} spectra of hydroxyferrocene and phenol. In each compound, the OH group is coplanar with the ring, while the IR frequencies are essentially the same, i.e., 3612 cm^{-1}. See ref 3a.

Chart 4

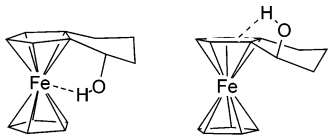

8 **9**

and the "trans" form **7b** with the OH group oriented away from the phenyl ring.[45] Due to the attractive electrostatic interactions between the OH group and the π-electrons, the minimum **7a** is more stable than the minimum **7b** lacking such interactions. The red-shift in the experimental OH stretching frequency on going from **7b** to **7a** (ca. 20 cm^{-1})[3,46] has been attributed to a weak OH$\cdots\pi$ interaction in conformer **7a**. The calculations for benzyl alcohol (and related aromatic compounds, see below) were undertaken at the BP86 level to gain insight into the accuracy of this DFT model used for predictions of stability and spectroscopic properties of the corresponding rotational isomers. At the BP86 level the calculated (unscaled) OH frequencies are 3605 and 3639 cm^{-1} in isomers **7a** and **7b**, respectively, in agreement with experimental results. In addition, at the BP86 level the form **7a** was calculated to be 1.1 kcal/mol more stable than the form **7b**, which is in agreement with earlier calculations at the MP2 and HF levels.[45] These results show that the BP86 model is capable of reproducing both the experimental and ab initio computational results for systems characterized by intramolecular OH$\cdots\pi$ interactions.

The assignment of the respective π-bonded (in **1c**) and metal-bonded (in **1a**) absorption bands of ferrocenyl alcohols is also supported by IR spectra of the isomeric *endo*- (**8**) and *exo*-1,2-(α-hydroxytetramethylene)ferrocene (**9**), in which only one each of the respective bonding modes is possible because of fixed *endo*- and *exo*-positions of the hydroxyl group on the nonrotating side chain (Chart 4). The *endo*-hydroxyl, suitably positioned for interaction with iron, gives rise to the lower frequency absorption peak, while the *exo*-hydroxyl produces the weaker, higher frequency.[47] We have optimized geometries of these two isomers at the BP86 level and calculated frequencies for **8** (ν_{OH} = 3563 cm^{-1}) and **9** (ν_{OH} = 3609 cm^{-1}) that are consistent with experimental data.

Isomer **8**, in which the OH group is orientated toward the metal, is calculated 1.1 kcal/mol more stable than **9**, which suggests that the stabilization effect of the OH$\cdots$Fe interaction is more important than that involving the π-system.

The time scale of IR spectroscopy is sufficiently fast for detection of individual constituents of an equilibrium mixture. That of NMR spectroscopy is much longer, so that simple rotamers cannot be resolved (unless separated by large barriers), and only averaged signals can be obtained. Nevertheless, additional evidence of *endo*- and *exo*-positions of the OH group in ferrocenyl-containing alcohols has been provided from conformational analysis based on the NMR chemical shifts of the protons of the unsubstituted cyclopentadienyl ring.[48] It has been shown that the relation between the averaged ^{1}H NMR chemical shifts of that ring ($\delta_{\text{"hetero"}}$) and the position of the OH group can be employed to deduce the preferred conformation in a series of ferrocenylcarbinols. According to this relation, the $\delta_{\text{"hetero"}}$ values of 4.2 and 4.0 ppm are indicative of *endo*- and *exo*-position of the OH group, respectively. Thus, for ferrocenylmethanol it was concluded that *endo*-orientation of the hydroxyl group is the most favorable (isomer **1a**), in agreement with the IR study[3] and our DFT calculations.

Table 2. Experimental and B3LYP//BP86 ^{57}Fe, ^{1}H, and ^{13}C NMR Chemical Shifts for Ferrocenylmethanol Isomers

rotamer	Fe[a]	C_1[b]	$C_{2/5}$	$C_{3/4}$	$C_{1'-5'}$	H_{OH}[b]	$H_{1'-5'}$
1a	2.5	93.2	68.6	68.0	68.2	2.1	4.2
1c	13.0	88.4	66.6	67.0	67.7	0.6	4.1
1d	−4.0	85.5	70.6	68.2	67.9	1.2	4.1
1e	21.6	87.8	66.4	67.1	68.5	1.3	4.3
expt[b]	−1.2	88.5	67.9	68.5	68.3	1.8	4.2

[a] Relative to ferrocene. [b] From ref 32.

NMR chemical shifts of ferrocenylmethanol isomers **1a**, **1c**, **1d**, and **1e** have been calculated at the B3LYP//BP86 level of theory (Table 2). In the case of ferrocenylmethanol **1a** the agreement between the calculated (relative to ferrocene as standard) and experimental values of ^{57}Fe, ^{1}H, and ^{13}C NMR chemical shifts is excellent. On the basis of the relative energy differences between the ferrocenylmethanol conformers (Table 1), one can estimate that contributions of other conformers **1c**, **1d**, and **1e** to the averaged chemical shifts of ferrocenylmethanol are relatively small.

Although the ^{57}Fe nucleus has a large chemical-shift range[49] and ^{57}Fe values can be very sensitive to slight changes in the geometry,[50] we found that the relative difference between calculated ^{57}Fe NMR chemical shifts in **1d** and **1e** (conformers with "free" OH group), **1c** (with OH$\cdots\pi$ interaction), and **1a** (with OH$\cdots$Fe interaction) is less than 30 ppm (Table 2). This suggests that intramolecular interactions between the OH group and the metal in **1a**, or between the OH group and the π-electrons in **1c**, are weak and cause only slight changes in the geometrical or electronic structure of the ferrocene core. For example, the difference between the average Fe−C distance in **1d** and **1a** is only 0.004 Å.

Since the intramolecular interaction between an OH group and a ruthenium center is stronger than the corresponding OH$\cdots$Fe interaction in ferrocenylmethanol analogues,[5] we have performed a comparative study for the $RcCH_2OH$ congener [Rc = $Ru(C_5H_5)(C_5H_4)$], for which three conformers, **1a**, **1c**, and **1d** (M = Ru, cf. Chart 2), can be located. The relative difference between the calculated ^{99}Ru NMR chemical shifts in **1a** (M = Ru) and **1d** (M = Ru) is more than 100 ppm. This value is much larger than the corresponding one for M = Fe, 7 ppm (Table 2), suggesting a stronger interaction in the ruthenocene than in the ferrocene derivative.[51] We also located the conformer **1c** (M = Ru) stabilized with an intramolecular OH$\cdots\pi$ interaction, which had not been described previously.[5] At the BP86 (B3LYP) level of theory this conformer is calculated to be 1.5 (0.9) kcal/mol less stable than **1a**, with the intramolecular OH$\cdots$Ru interaction.

(45) (a) Mons, M.; Robertson, E. G. Simons, J. P. *J. Phys. Chem. A* **2000**, *104*, 1430−1437. (b) Guchhait, N.; Ebata, T.; Mikami, N. *J. Am. Chem. Soc.* **1999**, *121*, 5705−5711.

(46) Visser, T.; van der Maas, J. H. *Spectrochim. Acta* **1986**, *42A*, 599−602.

(47) Trifan, D. S.; Bacskai, R., *Tetrahedron Lett.* **1960**, *13*, 1−8.

(48) Reich-Rohrwig P.; Schlögl K. *Monatsh. Chem.* **1968**, *99*, 2175−2186.

(49) See e.g.: *Transition Metal Nuclear Magnetic Resonance*; Pregosin, P. S., Ed.; Elsevier: Amsterdam, 1991.

(50) (a) Bühl, M.; Mauschick, F. T.; Terstegen, F.; Wrackmeyer, B. *Angew. Chem., Int. Ed.* **2002**, *41*, 2312−2315. (b) Wrackmeyer, B.; Tok, O. L.; Ayazi, A.; Maisel, H. E.; Herberhold, M. *Magn. Reson. Chem.* **2004**, *42*, 827−830.

(51) As far as the sensitivity of the central atom in the metallocenes toward geometrical distortions is concerned, that of ^{99}Ru is indicated to be less pronounced than that of ^{57}Fe, as judged from the computed shielding/bond-length derivatives, $\partial\sigma^M/\partial r_{M-Cp}$, −139.1 and −232.1 ppm pm^{-1} for M = Ru (this work) and Fe, respectively (Grigoleit, S.; Bühl, M. *Chem. Eur. J.* **2004**, *10*, 5541−5552).

Electron Density Topological and NBO Analyses

In the preceding section we have discussed energetic, IR, and NMR spectroscopic evidence for weak interactions between the OH group and the Fe atom (in **1a**) or the π-electrons (in **1c**). In the following, the nature of the OH···Fe interaction is studied in more detail, employing natural bond orbital (NBO) analysis and topological (Bader) analysis of the total electron density. In the latter, performed at the BP86 level using the Morphy97 program, no bond critical point (BCP) or atomic bond path between Fe and hydroxyl hydrogen atoms is found. This indicates that no classical hydrogen bond is formed. In addition, for interpretative purposes, Wiberg bond indices (WBIs)[52] for ferrocenylmethanol conformers were derived from the NBO analysis at the BP86 level. The calculated WBIs between the iron center and the hydroxyl hydrogen atom in **1a**, and between the C1 carbon atom and the hydroxyl hydrogen atom in **1c**, are 0.002 and 0.003, respectively, indicating negligible covalent contributions to OH···Fe and OH···π bonding interactions.[53] These findings are consistent with weak attractive forces that are predominantly electrostatic in nature, an interpretation that is further supported by the NPA atomic charges. For instance, on going from isomer **1d** with the "free" OH moiety to **1a**, the positive charge of the hydroxyl hydrogen increases slightly ($\Delta q = 0.01$), as does the negative charge of the metal atom ($\Delta q = -0.02$).

Similar results are obtained for $RcCH_2OH$, where the calculated Wiberg bond index between the Ru center and the hydroxyl hydrogen in **1a** (M = Ru) is 0.01. This value is 5 times larger than the one calculated for ferrocenylmethanol **1a** (M = Fe), indicating again that the OH···Ru interaction is stronger, but still too small to be interpreted as a OH···Ru hydrogen bond.[5] For comparison, at the BP86 level the topological analysis was performed for the ruthenocene derivative, but no bond critical point between ruthenium and hydroxyl hydrogen atoms was found, suggesting that both the OH···Fe (in **1a**, M = Fe) and OH···Ru (in **1a**, M = Ru) intramolecular interactions are of the same nature.

Likewise, no BCP is found between H and Fe in C_s-symmetrical **1b** (M = Fe), with an OH···Fe distance of 2.639 Å at the BP86 level. Interestingly, a BCP is found between the hydroxyl hydrogen and the C−$H_{1'}$ atom in **1b**, consistent with the short nonbonded H···H distance of 1.933 Å.[54] The characteristics of this BCP,[55] however, are indicative of a repulsive closed-shell interaction.

To estimate the critical distance between metal and hydroxyl hydrogen atoms at which the intramolecular hydrogen bonding OH···M can occur, partial geometry optimizations were performed for **1a** (M = Fe or Ru) with the M−H distance fixed to different values (ranging from 2.95 to 1.80 Å). According to topological analyses of the BP86 total electron density in these constrained structures, distances of 2.3 and 2.5 Å are necessary for M = Fe and Ru, respectively, for hydrogen bonding between metal and hydroxyl hydrogen atoms to be operative. In geometries with these (or lower) distances, BCPs between metal and hydroxyl hydrogen atoms appear, which are not present in the corresponding fully optimized geometries. In the case of ferrocenylmethanol (d(Fe···H) = 2.3 Å), this BCP is characterized by values of 0.025 and 0.050 au for the electron density (ρ) and its Laplacian ($\nabla^2\rho$), respectively, consistent with the existence of intramolecular hydrogen bonds.[56] With decreasing Fe−H distance in **1a** (M = Fe) both $\nabla^2\rho$ and ρ values increase, indicating stronger interaction. For instance, in the structure with an Fe−H distance of 2.0 Å, $\nabla^2\rho$ and ρ are increased to 0.060 and 0.042 au, respectively. It has been shown that ρ is related to the bond order and thus to the bond strength.[57]

Chart 5

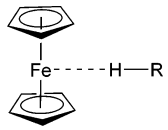

10 R = OH
11 R = F
12 R = OCF_3

The structure with the fixed Fe−H distance of 2.3 Å in **1a** (M = Fe) was found 7.8 kcal/mol above the corresponding unconstrained geometry (with an Fe−H distance of 2.949 Å). In the case of **1a** (M = Ru) the structure with the fixed Ru−H distance of 2.5 Å was found to be only 1.4 kcal/mol less stable than the corresponding fully optimized geometry (where the Ru−H distance is 2.785 Å). Thus, efficient OH···Fe hydrogen bonding would require large geometrical distortions in ferrocenylmethanol, but much smaller ones in the Ru congener, where the nature of the OH···Ru interaction is much closer to that of a normal hydrogen bond.

With a decreasing Fe−H distance in **1a**, the O−H bond becomes successively elongated, and the Fe···H−O bond angle becomes increasingly linear (see Figure S1 in the Supporting Information). These changes in geometrical parameters are also in agreement with hydrogen-bond formation. Interestingly, the O−H distance in **1a** (M = Fe), 0.983 Å, is already slightly longer than that in **1d**, the conformer with a "free" OH group (0.979 Å), but still much shorter than that in the constrained geometry with d(Fe−H) = 2.3 Å, where the OH distance is 1.000 Å.

Concomitant with this OH bond elongation, the BP86-calculated OH-stretching frequency for the hydroxyl group is increasingly red-shifted with smaller values of the fixed Fe−H distance. Also, we have found that the calculated ^{57}Fe NMR shielding is significantly perturbed by this "enforced" intramolecular OH···Fe hydrogen bond. On going from the fully optimized structure **1a** (stabilized by a weak intramolecular OH···Fe interaction) to the corresponding structure partially optimized with the fixed Fe−H distance of 2.3 Å (characterized by an intramolecular OH···Fe hydrogen bond), the ^{57}Fe nucleus is deshielded by ca. 190 ppm. This shift, however, may to a large extent be an indirect effect from the geometrical distortions in the constrained geometry.

To assess the intrinsic properties of an intramolecular OH···Fe interaction, unperturbed by constraints from the methylene tether in ferrocenylmethanol, we have studied the corresponding complexes of ferrocene with three small proton donors, H_2O, HF, and CF_3OH (see Chart 5). In the fully optimized

(52) Wiberg, K. *Tetrahedron* **1968**, *24*, 1083−1096.

(53) For comparison, the calculated WBI in the water dimer (H_2O···HOH) is 20−30 times larger than the corresponding values in the ferrocenylmethanol conformers.

(54) This value is in a range where intramolecular dihydrogen bonding could be operative (1.6−2.1 Å). (a) Popelier, P. L. A. *J. Phys. Chem. A* **1998**, *102*, 1873−1878. (b) Epstein, L. M.; Shubina E. S. *Coord. Chem. Rev*. **2002**, *231*, 165−181.

(55) The values of ρ and $\nabla^2\rho$ are 0.014 and 0.070 au. Also, the staggered C_s-symmetrical form (which has no BCP between H atoms) is only 0.4 kcal/mol above eclipsed **1b**; this value is smaller than the intrinsic rotational barrier in ferrocene (ca. 1 kcal/mol), suggesting that there is no attractive H···H interaction in **1b**.

(56) Koch, U.; Popelier, P. L. A. *J. Phys. Chem*. **1995**, *99*, 9747−9756.

(57) Wiberg, K. B.; Bader, R. F. W.; Lau, C. D. H. *J. Am. Chem. Soc*. **1987**, *109*, 1001−1012.

Chart 6

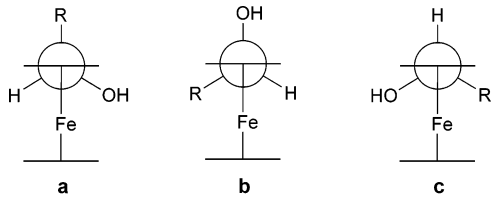

2 R = Me
3 R = *t*-Bu

complexes between ferrocene and water (**10**), HF (**11**), or CF_3OH (**12**) the optimized Fe···H distances are 2.763, 2.363, and 2.399 Å, respectively. These values are considerably shorter than that in ferrocenylmethanol **1a** (2.949 Å), but still too long for hydrogen bonding to occur, as confirmed by topological analyses in these three complexes.

The interaction energies between ferrocene and these protic donors are small, e.g., −1.9 kcal/mol for water, which is reduced to −1.2 kcal/mol after BSSE correction. Relative energies of ferrocene-containing alcohols with an OH···Fe interaction and with a dangling OH bond may thus be somewhat affected from BSSE, but not to an extent that would change the relative order of stability of these isomers or the general qualitative conclusions.[58]

Substituent Effects

It has been shown that substitution at the carbinol C_α atom in ferrocenylmethanol causes conformational differences due to increased steric hindrance.[4] However, conformational analysis performed earlier[4] with molecular mechanics methods may not be adequate to properly account for the steric and, in particular, the electronic features of rotational isomers in ferrocenylmethanol.[59]

The representation of the π-bonding between the metal and cyclopentadienyl rings is a major problem in modeling metallocenes, as commercially available force fields usually do not cater well to organometallic molecules.[59,60] In the rigid body approach applied earlier, the cyclopentadienyl ligand was treated as a rigid unit where bond lengths and angles were fixed during minimization.[4] Thus, interactions between metal and the cyclopentadienyl ligands were not considered. For ferrocenylmethylcarbinol (**2**) three different minima were located, and for *tert*-butylferrocenylcarbinol (**3**) only one possible conformation was obtained from MM calculations.[4]

Three conformations (**a**, **b**, and **c**) with respect to the rotation about the central C_1-C_α bond (ω) are conceivable (Chart 6). In addition, the OH group is free to rotate about the $O-C_\alpha$ bond (ϕ) to give three further rotational isomers in each confomer **a**, **b**, or **c**. Accordingly, a total of nine conformations are possible for both **2** and **3**, out of which we could locate seven and six, respectively, at the BP86 level.[61] The relative energy differences between the minima calculated with the MM method are only qualitatively consistent with our BP86 values. Whereas, for example, three MM-derived minima for **2** are within 1 kcal/mol of each other, seven BP86-optimized structures span a range of ca. 3 kcal/mol (Table 3).

Table 3. Relative Energies (kcal/mol) and Corresponding Angles (deg) Calculated at the BP86 Level for Ferrocenylmethylcarbinol (2) and *tert*-Butylferrocenylcarbinol (3) Isomers

R = Me	ω^a	ϕ	ΔE	R = *t*-Bu	ω	ϕ	ΔE
2a$_1$	−38.8	−42.8	0	**3a$_1$**	−36.5	−38.8	0
2c$_1$	−36.7	170.2	1.0	**3c$_1$**	−34.9	179.6	2.3
2b$_1$	67.5	55.6	1.4	**3b$_1$**	50.1	47.3	5.2
2b$_2$	82.6	−46.2	1.3				
2a$_2$	−142.1	45.6	0.9	**3a$_2$**	−130.4	36.4	3.9
2c$_2$	−143.8	−169.5	2.7	**3c$_2$**	−132.2	−159.9	6.4
2b$_3$	74.1	−178.9	2.9	**3b$_3$**	49.9	−166.6	6.7
expt[b]	76.2	−94.1		expt[c]	−40.3	-	

[a] Angles defined for the torsion about $C_2-C_1-C_\alpha-O$ (ω) and $C_1-C_\alpha-O-H$ (ϕ) bonds (ferrocene numbering defined in Chart 1). [b] From ref 41b. [c] From ref 41c.

In conformations **a** and **c**, OH···Fe intramolecular interactions are possible, depending on the angle ϕ. Conformation **a** is sterically more favorable than conformation **c** since the bulky alkyl groups prefer the *exo*-position, i.e., the position above the cyclopentadienyl ring. Conformation **b** would allow the occurrence of an OH···π intramolecular interaction, also depending on ϕ. Both in **2** and **3**, conformations **a** with $\phi = -42.8°$ and −38.8°, respectively ("gauche" rotamers), were found to be the most stable (Table 3). These conformers are stabilized by OH···Fe intramolecular interactions, analogously to conformer **1a** of ferrocenylmethanol (Chart 2). However, conformers **b** ($\phi = 55.6°$ and 47.3° for **2** and **3**, respectively), with the OH group rotated toward the cyclopentadienyl ring, were calculated to be less stable that the corresponding "free" rotamers (**2c$_1$** and **3c$_1$**), in which the OH group is unperturbed by any intramolecular interaction. Apparently, bulky substituents at the carbinol C atom (Me, *t*-Bu) cause a steric crowding, which imposes limitations on the formation of OH···π intramolecular interactions in conformer **b**. As a result, conformation **b** of both **2** and **3** with the OH group above the cyclopentadienyl ring becomes less favorable.

With increasing size of the substituent (R = H, Me, *t*-Bu), the Fe···H distance becomes shorter and the corresponding Fe−H−O angle becomes more linear. In conformers **1a** (R = H), **2a$_1$** (R = Me), and **3a$_1$** (R = *t*-Bu) the Fe···H distances are 2.949, 2.898, and 2.843 Å, respectively, and the Fe−H−O angles are 120.7°, 123.3°, and 128.8°, respectively. Thus, bulkier substituents in the conformation **a** favor intramolecular OH···Fe interactions, which is consistent with earlier experimental studies on spectral properties and reactivities of substituted ferrocenyl carbinols.[62] It is also consistent with the X-ray diffraction data, which indicate that monosubstituted ferrocenes with bulky groups at the carbinol C atom (e.g., phenyl, benzyl, or bicyclic substituents) are characterized by the shortest Fe···O and Fe···H distances.[63]

We have also investigated a series of ferrocenyl-containing alcohols **4**−**6** (Chart 1), where the OH group is separated from the ferrocenyl moiety by alkyl chains of increasing chain length, $-(CH_2)_n-$ ($n = 1-4$). As n increases, the number of rotational degrees of freedom increases, thereby increasing the volume space available to the OH group relative to the bonding sites,

(58) This notion is supported by the fact that at the CP-opt level, which is inherently free of BSSE, a comparable ferrocene + water interaction energy, −0.9 kcal/mol, and very similar relative energies for **1a**−**e** compared to those from Table 1 are obtained.

(59) Fey, N. *J. Chem. Technol. Biotechnol*. **1999**, *64*, 852−862.

(60) (a) Rappe A. K.; Colwell C. S.; Casewitt C. J. *Inorg. Chem*. **1993**, *32*, 3438−3450. (b) Timofeeva, T. V.; Lii, J.-H.; Allinger, N. L. *J. Am. Chem. Soc*. **1995**, *117*, 7452−7459.

(61) However, some of the rotamers converged back to **a**, **b**, or **c** conformation.

(62) Hon, F. H.; Tidwell, T. T. *J. Org. Chem*. **1972**, *37*, 1782−1786.

(63) See e.g.: (a) Ferguson, G.; Gallagher, J. F.; Glidewell, C.; Zakaria, C. M. *Acta Crystallogr., Sect. C: Cryst. Struct. Commun.* **1993**, *49*, 967−971. (b) Skibar, W.; Kopacka, H.; Wurst, K.; Salzmann, C.; Ongania, K.-H.; de Biani, F. F.; Zanello, P. Bildstein, B. *Organometallics* **2004**, *23*, 1024−1041. (c) Dimitrov, V.; Linden, A.; Hesse, M. *Tetrahedron: Asymm.* **2001**, *12*, 1331−1335.

Chart 7

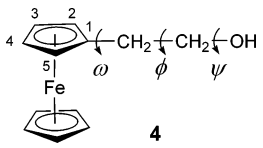

4

Table 4. Relative Energies (kcal/mol) and Corresponding Angles (deg) Calculated at the BP86 Level for Ferrocenylethanol (4) Isomers

rotamer	ΔE	ω^a	ϕ	ψ
4a	0	−162.4	61.0	−49.4
4b	0.1	90.9	60.6	−59.6
4c	0.3	87.0	177.2	63.6
4d	0.6	96.7	69.5	−167.7
4e	0.8	87.0	−179.9	179.9
4f	1.0	93.7	62.7	62.8
4g	1.1	−155.1	176.3	62.1
4h	1.2	−154.8	179.6	179.5
4i	2.6	−172.0	69.0	−178.8
expt[b]		74.7	174.0	27.6

[a] Angles defined for the torsion about $C_2-C_1-C_\alpha-C_\beta$ (ω), $C_1-C_\alpha-C_\beta$-O (ϕ), and $C_\alpha-C_\beta-O-H$ bonds (ferrocene numbering defined in Chart 7). [b] From ref 41a.

i.e., cyclopentadienyl ring and Fe center. Although these effects increase the statistical difficulty of maintaining the proximity of the interacting centers (intramolecular OH···Fe and OH···π interactions), there is still a detectable intramolecular OH···Fe interaction even in 4-ferrocenylbuthanol ($n = 4$).[3]

In 2-ferrocenylethanol (**4**, $n = 2$, Chart 7), the next higher homologue of ferrocenylmethanol ($n = 1$), the "free" and π-bonded OH-stretching frequencies in the IR spectrum are observed at 3636 and 3607 cm^{-1}, which is nearly equal to the frequencies in the structurally related 2-phenylethanol (3635 and 3606 cm^{-1}).[3] The electronic similarity of phenyl and ferrocenyl rings was confirmed again at the BP86 level by comparing calculated conformational and spectral properties of 2-phenylethanol and 2-ferrocenylethanol. The results obtained complement the similar comparative study performed for benzyl alcohol and ferrocenylmethanol isomers (see above), as well as earlier computational studies on conformational and spectral properties of 2-phenylethanol.[64] For the latter, five stable conformers were identified. The same types of conformers were found for 2-ferrocenylethanol (Table 4), namely, three conformers, **4b**, **4d**, and **4f**, corresponding to gauche structures with a folded side chain, and two conformers, **4c** and **4e**, representing anti conformers with extended side chains. In addition, four more conformers, **4a**, **4g**, **4h**, and **4i**, were located for 2-ferrocenylethanol, all characterized by an *endo*-position of the $-CH_2OH$ group. Conformers **4a** and **4b** are the most stable due to the presence of an intramolecular OH···Fe and OH···π interactions, respectively.

The third experimental band in the ν_{OH} region occurring at 3538 cm^{-1} has been attributed to an OH moiety interacting with the iron center. Thus, both OH···Fe and OH···π intramolecular interactions are operative in 2-ferrocenylethanol.

Isomer **4a**, stabilized by an intramolecular OH···Fe interaction, is calculated to be 0.1 and 0.3 kcal/mol more stable than isomer **4b**, which is stabilized by an intramolecular OH···π interaction, and the "free" isomer **4c**, respectively. The latter has been characterized by X-ray crystallography in the solid,[41a]

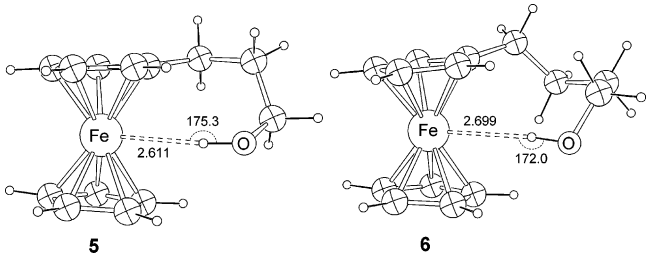

5 **6**

Figure 2. BP86-optimized geometries (O−H bonds and Fe···H distances in Å, angles in deg) of 3-ferrocenylpropanol (**5**) and 4-ferrocenylbutanol (**6**).

where it is probably stabilized by intermolecular hydrogen bonds (cf. the CPMD result for **1a** in water discussed above). Isomer **4a** is characterized by an Fe···H distance of 2.737 Å, which is 0.212 Å shorter than the corresponding distance in the ferrocenylmethanol isomer **1a** (Chart 2). This shows that elongation of the side chain facilitates the approach of the OH group toward the Fe center.

The experimental IR data for 2-ferrocenylethanol are well reproduced at the BP86 level. The corresponding vibrations in the ν_{OH} region obtained from the frequency calculations are 3529, 3581, and 3636 cm^{-1} (not scaled) for **4a**, **4b**, and **4c**, respectively, which is in good agreement with experiment. The difference between **4a** and **4c**, i.e., the red-shift upon formation of the OH···Fe interaction, exceeds 100 cm^{-1} and is almost twice as large as that in **1** (56 cm^{-1}, see Table 1). This interaction is thus much stronger in **4a** than in **1a**, consistent with the shorter Fe···H distance in the former than in the latter. However, the geometry of **4a** is still not optimal for formation of a true intramolecular hydrogen bond, as evidenced by topological analysis: No BCP was found between the Fe and hydroxyl hydrogen atoms, thus suggesting that only weak electrostatic Fe···H interactions are operative in **4a**.[65] This result is fully consistent with the analysis of the constrained geometries for **1a**, where an Fe−H distance as small as 2.3 Å is necessary for a classical hydrogen bonding to occur.

For the next homologues in this series, 3-ferrocenylpropanol (**5**) and 4-ferrocenylbutanol (**6**), a full conformational analysis becomes increasingly complex. We have limited ourselves to one representative conformer for each, which contains a OH···Fe moiety (Figure 2). The optimized Fe···H distances in **5** and **6** are 2.611 and 2.699 Å, respectively, revealing even closer contacts between Fe and hydroxyl hydrogen atoms than in **1a** or **4a**. As a consequence, even more red-shifted ν_{OH} bands are predicted for **5** and **6**, namely, 3497 and 3511 cm^{-1}, respectively. Even though the OH···Fe interaction appears to be even stronger in **5** and **6** than in the model H_2O adduct **10**, as judged from the shorter Fe···H distances in the former, no true hydrogen bond is to be expected in either case, as all Fe···H distances are well above the 2.3 Å threshold established above.

To explore how the OH···Fe interaction could be further reinforced, we finally studied an *ansa*-derivative with an ethylene spacer between the Cp rings, hoping that the concomitant tilt between these rings would cause a polarization of the d-orbitals at Fe such that electrostatic or specific MO interactions

(64) (a) Patey, M. D.; Dessent, C. E. H. *J. Phys. Chem. A* **2002**, *106*, 4623−4631. (b) Guchhait, N.; Ebata, T. Mikami, N. *J. Am. Chem. Soc.* **1999**, *121*, 5705−5711. (c) Mons, M.; Robertson, E. G.; Simons, J. P. *J. Phys. Chem. A* **2000**, *104*, 1430−1437.

(65) Note that the absence of a bond path does not mean the absence of any interaction, but rather the absence of interactions strong enough to leave their imprint on the topology of the electron density. The latter, in our case, appears to be quite insensitive to the basis set employed on the OH moiety: we performed additional geometry optimizations for **1a**, **4a**, and **5** using the 6-31G** basis on OH, i.e., with a set of polarization functions on the critical H (for **1a** also with 6-311G** and 6-311+G** on this moiety); in no case did topological analysis show a bond path between OH and Fe.

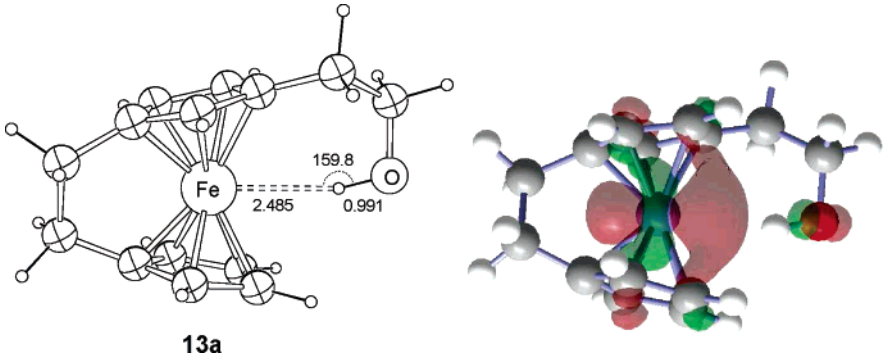

13a

Figure 3. BP86-optimized geometry (O−H and Fe···H distances in Å, angles in deg) of *ansa*-2-ferrocenylethanol **13a** (left) and plot of the second-highest MO (right).

with an OH group would be favored. *Ansa*-ferrocenes (or [*n*]-ferrocenophanes) are well known as precursors for ferrocene-based polymers,[66] and many have been characterized by X-ray-crystallography.[67] On the basis of the shorter Fe···H distance in 2-ferrocenyl ethanol **4a**, as compared to that in **1a**, we optimized the *ansa*-analogue **13a** (Figure 3), which is to our knowledge as yet unknown.

As expected, the OH···Fe interaction appears to be stronger in **13a** than that in **4a**, as evidenced by the short Fe···H distance of less than 2.5 Å (Figure 3) and the strongly red-shifted OH stretching frequency of 3413 cm^{-1} in the *ansa* species. Interestingly, even though the Fe···H distance is above the 2.3 Å threshold, topological analysis confirms the presence of a bond path and a BCP between both atoms ($\rho = 0.017$ au, $\nabla^2\rho = 0.037$ au).[68,69] The OH···Fe interaction in **13a** may thus be on the borderline to a true hydrogen bond. Inspection of the frontier MOs of **13a** reveals that the HOMO-1, which is mainly a d-orbital on Fe, has a noticeable p-character on the O atom, indicative of a mixing between d(Fe) and σ^*(OH) orbitals (see right-hand side of Figure 3). Also, the WBI between Fe and H is 0.01, significantly increased over that in **1a** (where it is 0.002; see the section on topological and NBO analysis above).

However, this apparent reinforcement of OH···Fe interaction in **13a** translates only into a weak extra energetic stabilization: We have optimized two other rotamers, **13b** and **13c** (not shown), corresponding to the conformations as in **4b** and **4c** with an OH···π interaction and a dangling OH bond, respectively. At the BP86 level, **13b** and **13c** are 1.4 and 2.6 kcal/mol, respectively, above **13a**.[70] While the energetic separation between these different bonding motifs is thus somewhat larger in **13** than in **1** or **4** (see Tables 1 and 4), the intramolecular OH···Fe interaction in **13a** would still be too weak to compete with typical H-bond acceptors. This notion is corroborated by a CPMD simulation of **13a** in water (similar to that of **1a**, but with 59 water molecules in the box), where the OH···Fe contact was lost after 2 ps, when the OH group reoriented itself and formed a H-bond to a water molecule from the bulk. Thus, *ansa*-derivatives such as **13** are promising candidates for the detection of intramolecular OH···Fe interactions, but only under the special conditions of low concentration in unpolar solvents.

Conclusions

We have presented a DFT-based conformational analysis of a number of ferrocene-containing alcohols, calling special attention to specific intramolecular interactions between the OH bond and the metal atom or the π-electrons of the cyclopentadienyl ligands. We find that conformers with an OH···Fe interaction are invariably the most favorable structure of a given compound, more stable by at least 1 kcal/mol than alternative forms with an OH···π interaction or a "free" OH group. In accordance with experimental IR data, the ν_{OH} stretching vibration is a very sensitive probe for the presence of such interactions, which manifest themselves in characteristic red-shifts of this band under suitable conditions. The strongest red-shifts of this band, up to ca. 100 cm^{-1} in unconstrained ferrocene-containing alcohols, are associated with conformers displaying the OH···Fe interaction.

Can this OH···Fe interaction be called a hydrogen bond? In monosubstituted ferrocene derivatives, rather long Fe···H distances between 2.61 and 2.95 Å are obtained. In these cases, very low bond orders are computed from natural population analysis, and in topological (Bader) analyses, no bond paths and bond critical points are found between the Fe and H atoms in question. In particular the latter criterion argues against the presence of OH···Fe hydrogen bonds, and the weakly stabilizing interaction between both moieties is probably just electrostatic in nature. According to model calculations with constrained geometries, Fe···H distances as short as 2.3 Å may be required for the occurrence of a bond path between both atoms. The gain in stabilization by such a close approach, however, is outweighed by increasing strain or repulsive interactions elsewhere in the molecule. When these factors are reduced or counterbalanced by additional attractive MO interactions, as in an *ansa*-ferrocenylethanol derivative with tilted cyclopentadienyl rings, the alcoholic H atom can approach the metal even closer, to ca. 2.5 Å. In that case, a bond path is found between both atoms, suggesting that the borderline to genuine OH···Fe hydrogen bonds could be reached with such a structural motif.

When potential H-bond acceptors are available in the vicinity, e.g., in the solid or in a suitable polar solvent, the intramolecular OH···Fe interaction cannot compete with intermolecular OH···X hydrogen bonds. This situation has been modeled in CPMD simulations of aqueous solutions, where the correspond-

(66) See e.g.: (a) Nguyen, P.; Gomez-Elipe, P.; Manners, I. *Chem. Rev.* **1999**, *99*, 1515−1548. (b) Abd-El-Aziz, A. S.; Todd, E. K. *Coord. Chem. Rev.* **2003**, *246*, 3−52.

(67) For example, the parent [2]ferrocenophane: Nelson, J. M.; Nguyen, P., Petersen, R.; Rengel, H.; Macdonald, P. M.; Lough, A. J.; Manners, I.; Raju, N. P.; Greedan, J. E.; Barlow, S.; O'Hare, D. *Chem. Eur. J.* **1997**, *3*, 573−584.

(68) The presence of such a BCP and the same values for ρ and $\nabla^2\rho$ are also obtained when the augmented 6-31+G(d,p) basis is used for the OH group in the geometry optimization, even though the optimized Fe···H distance is somewhat elongated to 2.539 Å.

(69) Similar values for ρ and $\nabla^2\rho$ have been obtained for complexes between $[Co(CO)_4]^-$ and hydrogen-bond donors: Alkorta, I.; Rozas, I.; Elguero, J. *J. Mol. Struct. (THEOCHEM)* **2001**, *537*, 139−150.

(70) At the BSSE-free CP-opt level, the relative energies of **13a**, **13b**, and **13c** are 0, 1.3, and 2.2 kcal/mol, respectively.

ing rearrangement of the OH group happened on the sub-picosecond time scale in the case of ferrocenyl carbinol and within two picoseconds for the *ansa*-ferrocenylethanol derivative.

In the unconstrained ferrocene-containing alcohols, the presence or absence of an OH···Fe interaction has only relatively small effects on the computed ^{57}Fe chemical shift, which is usually very sensitive to small changes in the geometrical or electronic structure.

While our DFT-based conformational analysis of ferrocenyl carbinol (**1**) and 2-ferrocenyl ethanol (**2**) is consistent with all available experimental data, there are notable differences with respect to previous results from molecular mechanics calculations. Apparently, the shape of the corresponding potential energy surfaces arises from a subtle interplay between steric and electronic factors, producing little energetic discrimination between various conformers. This situation appears to be too demanding for present-day classical force fields for organometallic species, at least for the ferrocene-containing alcohols studied so far. On the other hand, electrostatic interactions can often be parametrized reasonably well classically. Adjusting, for instance, atomic charges in the parameter set might thus open an avenue for refining force fields, tailoring them for specific OH···metal interactions.

In summary, we have demonstrated that the electronic and geometrical structure, as well as spectroscopical properties of ferrocene-containing alcohols, can be very well described at an appropriate DFT level, the BP86 model in our case. This approach presents itself as the method of choice for further studies of weak OH···metal interactions and hydrogen bonds.

Acknowledgment. M.B. wishes to thank Prof. W. Thiel and the Max-Planck-Institut für Kohlenforschung for continuing support. A Humboldt fellowship for V.V. is gratefully acknowledged. Computations were performed on Compaq XP1000 and ES40 workstations as well as on an Intel Xeon PC cluster at the MPI Mülheim, and on an IBM p690 "Regatta" cluster at the Rechenzentrum Garching.

Supporting Information Available: Optimized coordinates of all species **1**−**6** discussed in the text, and graphical material illustrating the dependence of total energy, OH distance, Fe···H−O angle, and ν_{OH} frequency on the Fe···H distance in constrained optimizations of **1a**. This material is available free of charge via the Internet at http://pubs.acs.org.

OM050810P